Glabridin attenuates endothelial dysfunction and permeability, possibly via the MLCK/p-MLC signaling pathway

GANXIAN WANG[1*], GUANGCHENG SUN[1,2*], YI WANG[1], PEI YU[1], XUE WANG[1], BIRONG ZHOU[2*] and HUAQING ZHU[1]

[1]Laboratory of Molecular Biology and Department of Biochemistry, Anhui Medical University, Hefei, Anhui 230032; [2]Department of Cardiology, The First Affiliated Hospital of Anhui Medical University, Hefei, Anhui 230022, P.R. China

Received December 4, 2017; Accepted September 13, 2018

DOI: 10.3892/etm.2018.6903

Abstract. Atherosclerosis is caused by various factors, and Glabridin may have protective effects on the cardiovascular system. The purpose of the present study was to evaluate the effects of Glabridin on atherosclerosis and evaluate whether Glabridin attenuates arteriosclerosis and endothelial permeability by suppressing the myosin light chain (MLC) kinase (MLCK)/phosphorylated (p)-MLC system via the mitogen activated protein kinase (MAPK) signaling pathway. Male New Zealand rabbits were randomly divided into 3 groups: The control group was administered an ordinary diet, whereas the high fat group and the Glabridin (2 mg/kg/d) intervention group were administered a high fat diet. Following 12 weeks, the blood lipid levels of rabbits, the morphological structure of the arterial wall, the arterial intimal permeability, the endothelial function and the mRNA levels of MLCK were measured. Western blot analysis was used to detect the levels of MLCK, p-c-Jun N-terminal kinase (JNK), p-extracellular signal regulated kinase (ERK), and p-p38. The high-fat diet group exhibited significantly increased total cholesterol and triglycerides, and endothelial dysfunction, which were attenuated by Glabridin treatment. Notably, the aortic endothelial permeability was increased in the high-fat diet group but was ameliorated in the Glabridin treatment group. Hyperlipidemia enhanced the expression of p-MLC and MLCK, which were associated with the increased phosphorylation of ERK, p38 and JNK. These changes were also ameliorated by Glabridin. In conclusion, the results of the present study suggested that atherosclerosis may be associated with upregulated MLCK expression and activity, which was downregulated by Glabridin. The mechanism of action of Glabridin was thought to proceed through modulating MAPK pathway signal transduction. However, further studies are required to adequately illuminate the exact regulatory mechanisms involved.

Correspondence to: Dr Birong Zhou, Department of Cardiology, The First Affiliated Hospital of Anhui Medical University, 218 Jixi Road, Hefei, Anhui 230022, P.R. China
E-mail: zhoubirong1@hotmail.com

Professor Huaqing Zhu, Laboratory of Molecular Biology and Department of Biochemistry, Anhui Medical University, 81 Meishan Road, Hefei, Anhui 230032, P.R. China
E-mail: aydzhq@126.com

*Contributed equally

Key words: Glabridin, atherosclerosis, myosin light chain kinase, permeability

Introduction

Atherosclerosis is a main pathological basis of cardiovascular and cerebrovascular disease, such as coronary heart disease, ischemic cerebrovascular disease and thromboembolic disease (1). Atherosclerosis is a large and middle artery disease, a major cause of heart disease and stroke, and a chronic inflammatory disease induced by large amounts of lipid and cholesterol accumulated in the large and medium-sized arteries, and accompanied by fibrous plaque formation (2). Epidemiological studies (3,4) have demonstrated that certain environmental and genetic factors are associated with the occurrence and development of atherosclerosis. The main genetic factors include high density lipoprotein reduction, increased low density lipoprotein and very low density lipoprotein, elevated blood pressure and elevated blood sugar (5). In addition, there are certain major environmental factors, including a high-fat diet, smoking, lack of exercise, antioxidant levels and infectious disease (2).

Vascular endothelial cells not only constitute a semi-selective permeability barrier between blood and tissue fluid, but also synthesize and secrete a variety of bioactive substances. Their structural integrity and barrier function have a central role in maintaining cardiovascular homeostasis (6). It has been widely recognized that damaged blood vessel endothelium leads to endothelial dysfunction, further expression and release of various bioactive substances and adhesion molecules (2). These changes ultimately lead to the formation of atherosclerosis, which is a chronic inflammatory process (1). Vascular endothelial dysfunction is an early manifestation of atherosclerosis (7,8), promoting lipid deposits, monocytes under the endothelium and the formation of foam cells.

The maintenance of the normal barrier function of vascular endothelium is associated with the dynamic balance between

tight junctions (TJs), adherence junctions and cytoskeleton contraction (6). Cell contraction is a common way to increase barrier permeability. Cell contraction is mainly affected by actin and myosin, and endothelial permeability is increased when actin and myosin produce a greater contraction force (6). Myosin II includes a heavy chain and a light chain, and myosin light chain (MLC) is divided into the basic light chain and regulatory light chain. It is the regulatory light chain that serves a regulatory role in myosin activity (9). MLC kinase (MLCK), dependent on Ca^{2+}/calmodulin (CaM) binding protein kinase, is a member of the immunoglobulin superfamily and is activated by the regulatory light chain in MLC. When activated by certain factors, MLCK could induce phosphorylation of MLC and vascular endothelial cell cytoskeleton rearrangement (10). This induces the following effects: Concentric contraction of endothelial cells, the destruction of TJs between cells and vascular barrier dysfunction (11). Finally, the endothelial permeability increases, a large number of lipid components infiltrate and deposit under the endothelium which then affects vascular endothelial barrier function (12).

Glycyrrhiza uralensis Fisch is mainly from the West, including leguminous plants *Glycyrrhiza uralensis*, *Ural Glycyrrhiza uralensis*, *Glycyrrhiza glabra* and dry root and rhizome (13). Glabridin is extracted from Guangguo licorice, insoluble in water and has antioxidant, anti-inflammatory (14) and anti-atherosclerosis (15) properties, which provide rationale for its use as a treatment of cardiovascular disease.

In the present study, the association between the effect of Glabridin on atherosclerosis, and the mitogen-activated protein kinase (MAPK) signaling pathway and myosin light chain phosphatase-dependent MLC phosphorylation was investigated. The experiment was conducted by establishing an animal model of atherosclerosis, and analyzing blood lipid changes, and observing changes in vascular morphology, MLCK expression, and intimal permeability.

Materials and methods

Reagents. Glabridin was purchased from DC Chemicals (Shanghai, China). Cholesterol was obtained from China Pharmaceutical (Group) Shanghai Chemical Reagent Company (Shanghai, China). Normal rabbit feed was obtained from Experimental Animal Center of Anhui Medical University (Hefei, China). The Triglyceride assay kit (cat. no. 10018) and the Total Cholesterol assay kit (cat. no. 10028) were purchased from Zhejiang Dongou Biochemical Co., Ltd. (Zhejiang, China).

Animals and groups. A total of 18 3-month-old, male New Zealand white rabbits (2.4±0.5 kg) were purchased from Shandong Qingdao Kang group (Qingdao, China). Rabbits were housed at room temperature with a humidity of 50-60% and were subjected to a 12 h light/dark cycle, with free access to food and water. The rabbits were randomly divided into 3 groups and fed as follows: Control group (n=6), basic diet for 12 weeks; HF group (n=6), high fat diet for 12 weeks; and Glabridin treatment group (n=6), high fat diet with 2 mg/kg/day Glabridin via oral catheter from weeks 6-12. The Glabridin dose was selected on the basis of a preliminary experiment according to a previous study (16). High fat diet consisted of 1% cholesterol and 5% lard prepared in rabbit food. The cholesterol concentration was determined in accordance with previous literature (17).

For the determination of total cholesterol (TCH) and triglyceride (TG), the rabbits were fasted for 1 day. The rabbits were then anesthetized with 3% sodium pentobarbital (30 mg/kg; Sigma-Aldrich; Merck KgaA, Darmstadt, Germany), and GES6 color ultrasonic diagnostic apparatus was used to observe the abdominal aorta. Blood samples were taken from the abdominal aorta and following standing for 2 h at 37˚C, the blood was centrifuged for 10 min at room temperature at 1,006 x g. The supernatant was removed and stored at -80˚C.

A previous study was referenced to understand the structure of rabbit aortas (18). Following sacrifice, rabbit aortas were removed and divided into three parts. Each part had the same number of rabbit aortas from the control, treatment and high fat group. For part one, one abdominal aorta was randomly selected from each of the three groups. These aortas were fixed in 10% formalin at room temperature for 8 h, and embedded in paraffin for the immunohistochemical and morphological analysis. Another part was embedded in optimum cutting temperature compound (OCT), immediately at -80˚C prior to freezing, preparing for permeability analysis and oil red O staining. The third part of abdominal aortas was frozen immediately at -80˚C for western blot analysis. All experiments were approved by the Ethics Committee of Anhui Medical University.

Detection of serum lipids. The enzyme coupling colorimetric method was utilized to detect the TCH and TG in model rabbits. All protocols were performed in strict accordance with the assay kits and ELISA instructions.

Endothelial function assay. The endothelial function assay was performed as described previously (17). Rabbits were anesthetized using 3% sodium pentobarbital (30 mg/kg), and the abdomens were shaved. The abdominal aorta was observed using a GES6 color ultrasonic diagnostic apparatus and 13-Mhz ultrasound probe. The probe was placed 0.5-1.0 cm below the renal artery to obtain a longitudinal axis view of the abdominal aorta. The basal diastolic diameter (D_0) of the abdominal aorta was measured initially, followed by the maximum diameter of the end diastolic (D_X) of the abdominal aorta after the left hind limb was compressed for 5 min. During the process, the probe position was maintained. Maximum diastolic rate of abdominal aorta in each rabbit (%) was calculated as follows: $(D_X-D_0)/D_0$ x100%.

Permeability assay. The permeability assay using the surface biotinylation technique was performed as described by Wang *et al* (19) with modifications specifically for the aortic intima. The abdominal aorta canals were filled with a Sulfo-NHS-LC-Biotin solution (Pierce; Thermo Fisher Scientific, Inc.) in HBS at 1 mg/ml for 30 min at room temperature. Aortas were then rinsed with PBS, embedded in OCT, and cryosectioned. Subsequently, the 6-μm frozen sections were incubated in 5% skimmed milk powder at 4˚C overnight. Following washing 3 times with PBS, the sections were incubated at 4˚C overnight with Rhodamine 600 Avidin

D (XRITC-avidin; 1:200; cat. no. A-2005; Shanghai Haoran Biological Technology Co., Ltd., Shanghai, China). The samples were then examined by fluorescence microscopy (magnification, x400). Images were captured, and the JD-801 Pathological Image Analysis system 4.0 (Jiangsu JEDA Science-Technology Development Co., Ltd., Jiangsu, China) was used to measure the integral optical density values.

Histological examination. Abdominal aorta specimens were dehydrated and embedded in paraffin, sectioned (4 μm) and stained with hematoxylin and eosin as previously reported (20). Extracellular matrix deposition was assessed using Masson trichrome staining, via the sequential addition of Bouin (at 25˚C for 24 h), Weigert (at 25˚C for 5 min), and Biebrich (at 25˚C for 5 min) solutions (OriGene Technologies, Inc., Rockville, MD, USA) to sections, in accordance with the manufacturer's protocol provided by the supplier of Bouin, Weigert and Biebrich solutions.

Lipid and fat content was evaluated by oil red O staining. Frozen sections were fixed with 10% formalin for 30 min at room temperature. Following rinsing with 60% isopropyl alcohol for 5 min, filtered oil red O working solution was used to stain the aorta sections (4 μm) for 5 min at room temperature. Sections were rinsed again with distilled water to reduce the background, and imaged using light microscopy (magnification, x100). Images were captured, and the JD-801 Pathological Image Analysis system was used to measure the integral optical density values. Image-Pro Plus software 6.0 (Media Cybernetics, Inc., Rockville, MD, USA) was used to measure the area ratio. The area ratio (%) was calculated as follows: Plaque area/total arterial area x100%.

Immunohistochemistry analysis. The abdominal aorta tissues sections were deparaffinized, rehydrated, then fixed with a methanol -0.3% H_2O_2 solution at room temperature for 20 min. Following high compression heating at 60˚C, the abdominal aorta was immersed in xylene (I) for 5 min, xylene (II) for 5 min, 100% ethanol for 5 min, 95% ethanol for 2 min, 90% ethanol for 2 min, 85% ethanol for 2 min, 80% ethanol for 2 min, soaked in 75% ethanol for 2 min and washed using distilled water. Antigens were unmasked by cooling for 30 min at room temperature. Sections (4 μm) were then blocked using PBS containing 0.05% Tween-20 and 1% BSA (Sigma-Aldrich; Merck KGaA) at room temperature for 30 min. Primary antibodies against MLCK (1:1,000; M7905; Sigma-Aldrich; Merck KGaA) were incubated with the tissue sections at 4˚C overnight; subsequently, sequential incubation was performed with biotinylated secondary antibodies (1:1,000; cat. no. 211-032-171; AmyJet Scientific Inc., Wuhan, China) and horseradish streptavidin (Cusabio Technology LLC, Houston, TX, USA) for 30 min at 37˚C. Finally, the samples were incubated with diaminobenzidine together at room temperature for 2 min, and hematoxylin was used to counterstain the nuclei. Positive stained cells appeared brown in color. Images were captured using light microscopy (magnification, x400), and the JD-801 Pathological Image Analysis system was used to measure the integral optical density values.

Reverse transcription-quantitative polymerase chain reaction (RT-qPCR). Total RNA was extracted from the aorta using the Trizol reagent (Invitrogen; Thermo Fisher Scientific, Inc.). mRNA was then reverse transcribed into cDNA using the RT-qPCR reverse transcription kit (Takara Biotechnology Co., Ltd., Dalian, China) in accordance with the manufacturer's protocol. RNA expression was determined using RT-qPCR with the following primers: MLCK forward, 5'-TCTTGGGAG AGGATGACGAA-3' and reverse, 5'-GTGTGGCAGAGG GTGAGAAG-3'; GADPH forward, 5'-TCACCACCTTCT TGATGTCG-3' and reverse, 5'-TGAACGGGAAACTCACTG G-3'. The thermocycling conditions were as follows: Initial denaturation at 95˚C for 15 min; 40 cycles of denaturation at 95˚C for 10 sec, annealing at 60˚C for 30 sec and extention at 72˚C for 30 sec. The reaction mixture contained the following materials: 2X Power SYBR Green Master Mix (Applied Biosystems; Thermo Fisher Scientific, Inc.), cDNA template, 10 pmol/μl of each primer and sterile water. Using GraphPad Prism software version 5.01 (GraphPad Software, Inc., La Jolla, CA, USA), relative gene expression was quantified according to the comparative Cq method (21). With respect to the expression levels of GAPDH, all results were normalized. A reverse transcription kit was purchased from, and primers of MLCK and GAPDH were obtained from Shanghai Shenggong Biology Engineering Technology Service, Ltd. (Shanghai, China).

Western blotting. The levels of MLCK, phosphorylated (p)-c-Jun N-terminal kinase (JNK), p-extracellular signal regulated kinase (ERK) and p-p38 were measured by western blotting. The following antibodies ERK (cat. no. sc-135900), p-38 (cat. no. sc-7149), JNK (cat. no. sc-7345), MLCK (cat. no. sc-365352), p-JNK (cat. no. sc-6254), p-ERK (cat. no. sc-7976), β-actin (cat. no. sc-47778) and p-p38 (cat. no. sc-7975-R) were purchased from Santa Cruz Biotechnology, Inc. (Dallas, TX, USA). All were used at a dilution of 1:1,000. The experimental procedures were described in a previous study (22). Levels of β-actin were used to normalize the relative protein expression levels. Experiments were repeated three times independently. Western blotting images were analyzed using the quantity one image processing system 4.62 (Bio-Rad Laboratories, Hercules, CA, USA).

Statistical analysis. All statistical analyses were carried out using SPSS software, version 16.0 (SPSS, Inc., Chicago, IL, USA). All data are expressed as the mean ± standard deviations. Comparisons between groups were carried out using one-way analysis of variance followed by Student-Newman-Keuls method. $P<0.05$ was considered to indicate a statistically significant difference.

Results

Blood lipid analysis. Following 12 weeks of treatment, the TCH and TG in the high fat model group were significantly higher than those in the normal control group. Compared with the high-fat model group, Glabridin significantly reduced the serum TCH level, and the level of TG was markedly reduced (Table I).

Morphological characteristics. Following 12 weeks of high-fat diet intervention, the rabbit abdominal aorta was observed by

Table I. The effect of high fat diet and Glabridin on TCH and TG of atherosclerosis model rabbits.

Level	Control	High fat diet	Glabridin
TCH (mmol/l)	1.03±0.38	68.56±4.78[a]	52.90±9.3[b]
TG (mmol/l)	0.40±0.21	9.16±2.57[a]	6.45±2.68

[a]P<0.05 vs. control; [b]P<0.05 vs. high fat diet. TCH, total cholesterol; TG, triglyceride.

oil red O staining. As presented in Fig. 1A, atherosclerotic plaques were observed in the rabbit aorta of the high fat model group and Glabridin group in comparison with the normal control group. Plaques of the rabbit aorta in the high fat model group were more obvious than in the normal control group and Glabridin treatment group. Compared with the high-fat model group, the plaques of the high-fat group were decreased following treatment with Glabridin. The results of the integrated optical density and plaque area ratio also illustrate these findings (Fig. 1B and C).

Endothelial function. The effects of Glabridin on vascular endothelial function were evaluated. Following pressurization for 5 min, aortic vasodilatation function in the high-fat model group was poorer than the normal control group. The results were as follows: Normal group. The fundamental maximum diameters of the abdominal aortas were 2.65, 2.25, 2.42 and 2.25 mm; the maximum diameter of the abdominal aortas following pressuring left hind limbs for 5 min were 2.90, 2.43, 2.71 and 2.51 mm, which were increased by 9.43, 8.00, 11.98 and 11.56%, respectively, compared with the fundamental maximum diameter. Model group. The fundamental maximum diameters of the abdominal aortas were 2.07, 2.06, 2.59 and 1.81 mm; the maximum diameter of the abdominal aortas following pressuring left hind limbs for 5 min were 2.11, 2.10, 2.63 and 1.91 mm, which were increased by 1.93, 1.94, 1.54 and 5.52%, respectively, compared with the fundamental maximum diameter. Glabridin group. The fundamental maximum diameters of the abdominal aortas were 1.77, 1.96, 1.92 and 1.96 mm; the maximum diameter of the abdominal aortas following pressuring left hind limbs for 5 min were 1.86, 2.10, 2.06 and 2.06 mm, which were increased by 9.00, 7.14, 7.29 and 5.10%, respectively, compared with the fundamental maximum diameter. Compared with the high fat model group, the aortic vasodilatation rate was significantly increased in the Glabridin group (Fig. 2).

Endometrial permeability. In the normal control group, the structure of aortic intima was intact, and the endothelial cells were closely connected and arranged neatly. Compared with the normal control group, a large number of foam cells were observed in the aorta intima in the high-fat model group, and the aortic intima markedly thickened. However, in the Glabridin treatment group, both foam cells and aortic intima were markedly ameliorated. As presented in Fig. 3, fluorescence microscopy indicated that in the normal control group there was no fluorescent dye penetration, and in the high fat model group rabbit aortic permeability increased markedly, with fluorescent dye penetration throughout almost all layers of the wall. Following administration of Glabridin, a degree of permeability remained. However, the degree of penetration of fluorescent dyes was decreased in comparison with the high fat model group (Fig. 3).

Measurement of relative MLCK expression levels. As observed by immunohistochemical methods (Fig. 4A), following 12 weeks of diet intervention, high MLCK expression levels were observed in the arterial wall in the high fat model group, in the aortic intima-medias and smooth muscle layers, with a marked increase in comparison with the normal control group. In the Glabridin treatment group, this expression was markedly reduced, compared with the high fat diet group. The transcription level of MLCK was analyzed by RT-qPCR through. As presented in Fig. 4B, Glabridin significantly downregulated the transcription level of MLCK mRNA in comparison with the high fat diet groups, which was in accordance with the results of western blotting. Western blotting (Fig. 4C) demonstrated that following 12 weeks of high-fat diet intervention, compared with the normal control group, the expression level of MLCK protein increased, which was then downregulated by Glabridin.

Measurement of reactive signal pathway activity level. Western blotting revealed that the levels of phosphorylation of JNK, ERK and p38 were significantly enhanced in the high fat group, compared with the normal control group. However, the phosphorylation level of JNK, ERK, p38 in MAPK signaling pathway was significantly downregulated by Glabridin, in comparison with the high fat diet group (Fig. 5).

Discussion

Up to now, the study of atherosclerosis is not comprehensive. The changes in the different stages of atherosclerosis can be regarded as different stages of chronic inflammation. Various cellular responses are similar to the inflammatory response, which serves as the body's response to injury (23,24). The dysfunction of endothelial structure is the initial stage of atherosclerosis, followed by a series of inflammatory reactions, a large number of inflammatory factors released and promoting the further development of atherosclerosis (25). Endothelial cells serve an important role in regulating cardiovascular functions and systemic homeostasis and in regulating pathophysiological processes such as inflammation and immunity (26). Clinically, there is no effective drug for prevention and treatment.

New Zealand rabbits were used to establish an atherosclerosis model as the rabbit diet is sensitive to high cholesterol, and they typically have low levels of cholesterol in their blood plasma (27), which significantly increases following the administration of a high-cholesterol diet. Food-induced lesions are located in the aorta, and inflammatory cell infiltration, increased permeability of intima and a large number of macrophages differentiating into foam cells, are similar to those observed in humans (28).

The rabbit models of atherosclerosis were established through diet intervention for 12 weeks. The TCH and TG in

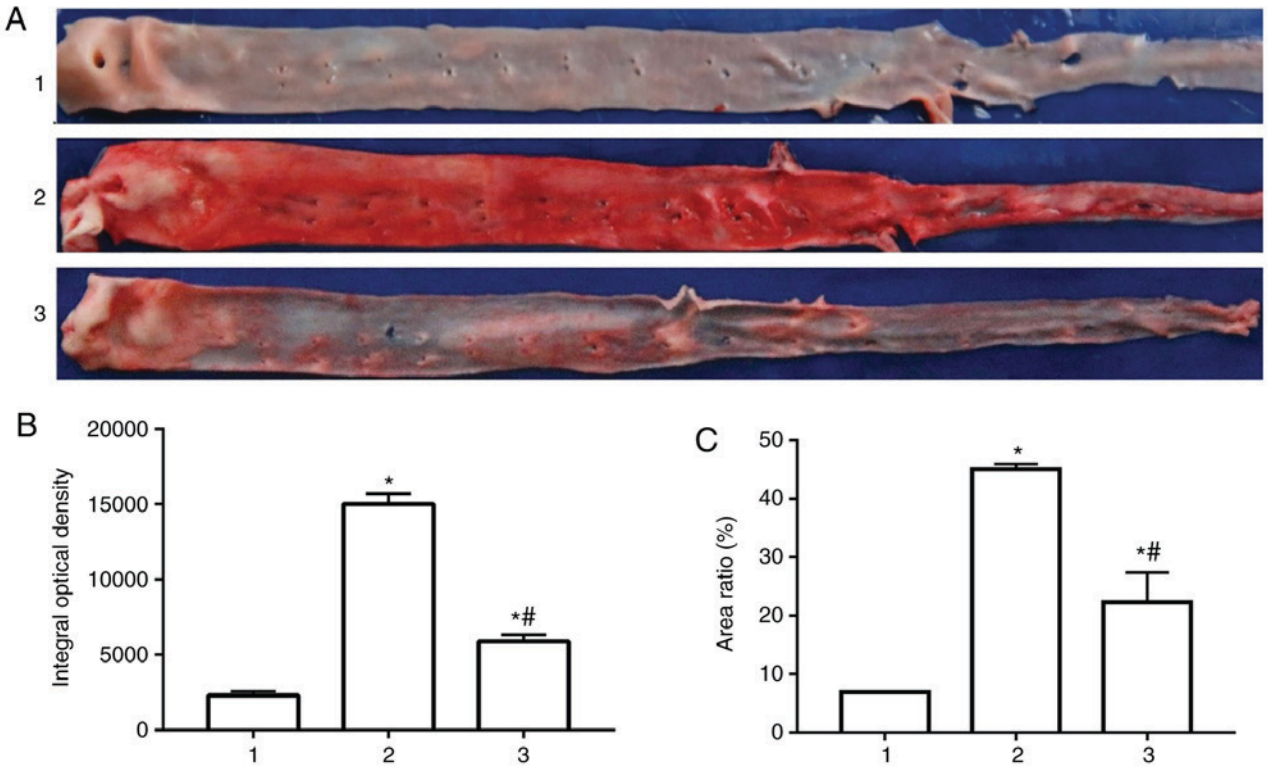

Figure 1. The effects of high fat diet and Glabridin on atherosclerotic lesions of aorta. (A) Oil red O-stained aortas. (B) Lipid quantification. (C) Plaque area ratio. Area ratio (%) = plaque area/total arterial area x100%. *P<0.05 vs. 1; #P<0.05 vs. 2. 1, normal group; 2, high fat diet group; 3, Glabridin group.

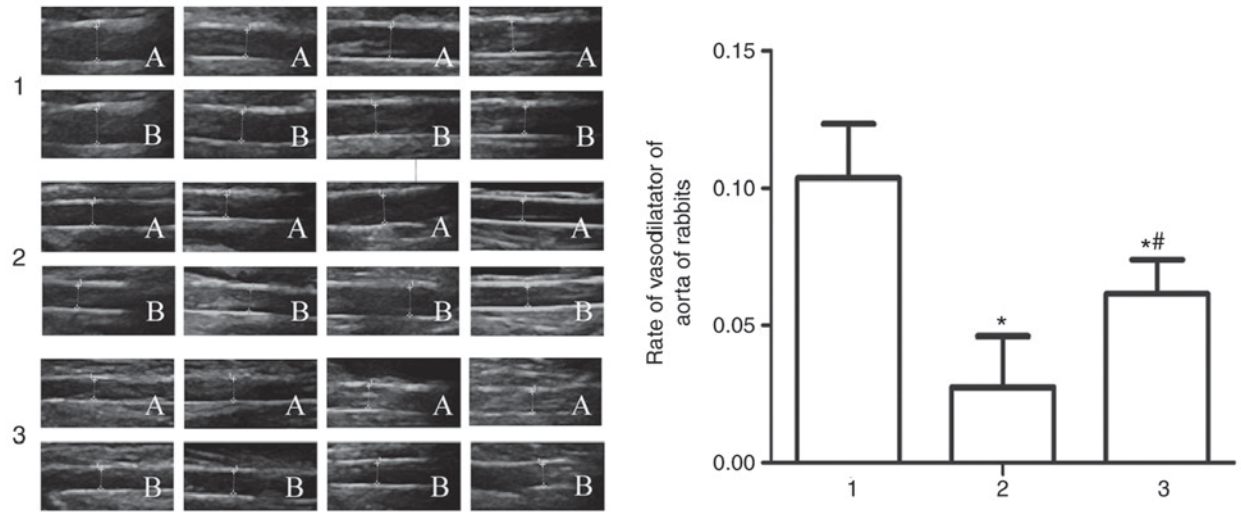

Figure 2. Effect of Glabridin on arterial endothelial function in atherosclerotic arteries. *P<0.05 vs. 1; #P<0.05 vs. 2. 1, normal group; 2, model group; 3, Glabridin group; A, the fundamental maximum diameter of the abdominal aorta; B, the maximum diameter of the abdominal aorta following pressuring left hind limb for 5 min.

the high fat model group were significantly higher than those in the normal control group, compared with the high-fat model group. Glabridin significantly reduced the serum TCH level and markedly reduced the level of TG.

Following diet intervention for 12 weeks, the expression of MLCK in the high fat group was significantly higher than the normal control group. Following Glabridin treatment, this was ameliorated, suggesting that Glabridin served a role in downregulating the expression of MLCK; as observed by immunohistochemistry and western blotting. The decrease of MLCK expression contributed to inhibiting the phosphorylation level of MLC, ultimately downregulating the vascular permeability. Increased vascular permeability is also an important factor in promoting atherosclerosis (29). In the present study, the permeability of arterial intima was detected by macromolecular fluorescent dye penetration. It was demonstrated that there was almost no osmotic dye in the aorta of rabbits in the normal group. Vascular permeability was

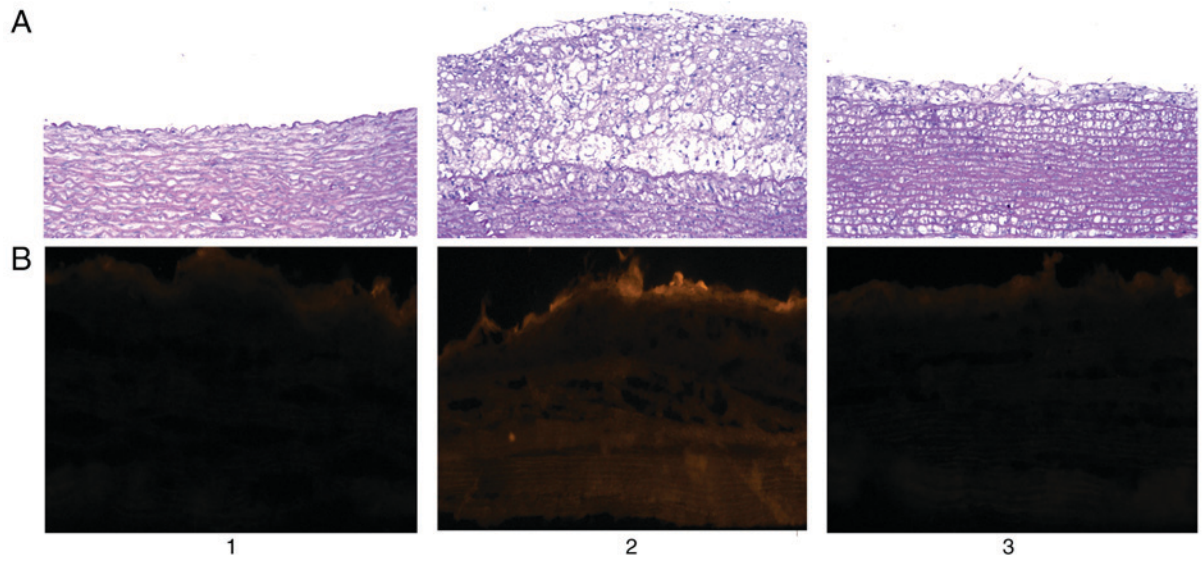

Figure 3. Effect of Glabridin on intima permeability of atherosclerotic arteries. (A) Rabbit arterial morphological structure visualized by hematoxylin-eosin staining (magnification, x100). (B) Permeability assay of rabbit aorta intima by surface biotinylation (magnification, x400). 1, normal group; 2, high fat diet group; 3, Glabridin group.

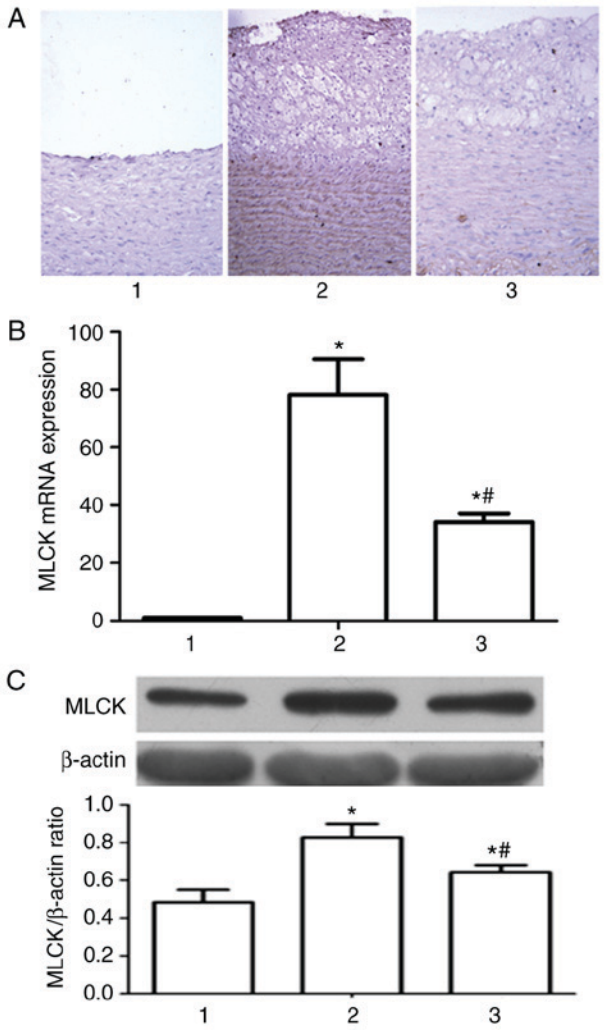

Figure 4. Effect of Glabridin on the expression of MLCK. (A) Representative immunohistochemical image (magnification, x400). (B) Reverse transcription-quantitative polymerase chain reaction results. (C) Western blotting results. *P<0.05 vs. 1; #P<0.05 vs. 2. 1, normal group; 2, model group; 3, Glabridin group; MLCK, myosin light chain kinase.

increased in the high-fat group, and the dye almost immersed into the whole layer. However, this phenomenon was markedly ameliorated by Glabridin, which indicated that Glabridin could ameliorate vascular permeability. Normal endothelial cells express a certain amount of MLCK, and the level of MLCK expression was increased following 12 weeks of high-fat diet intervention. The expression of MLCK promoted the phosphorylation of MLC, inducing vascular endothelial cell cytoskeleton rearrangement, resulting in vascular endothelial cells in concentric contraction, TJs between the endothelial cells were damaged, cell gaps increased, and finally, the permeability of endothelial cells increased. Increased endothelial cell permeability promotes lipid, monocytes and other depositions in the subcutaneous tissue, and contributes to the formation of foam cells and atherosclerotic plaque, leading to decreased vascular elasticity and diastolic function. The results of the abdominal aorta diastolic function measured by percutaneous ultrasonography were also consistent with the above results.

Considerable evidence has suggested that MAPK is associated with atherosclerosis (30-32). MAPK belongs is a serine/threonine protein kinase, and there are 4 MAPK pathways known at present, namely, ERK1,2; JNK/stress-activated protein kinase; p38 MAPK; and big mitogen activated protein kinase, in which ERK/MAPK is an important pathway. The four pathways activate the cascade reaction, that is, the kinase of MAPK kinase to the MAPK kinase to MAPK (30). The MAPK signaling pathway includes the activation of p38/MAPK, ERK/MAPK and JNK/MAPK, and is associated with the induction of inflammatory factors (33). The present study suggested that the phosphorylation levels of p38, ERK and JNK were increased in the high fat group, but decreased by Glabridin. This suggests that Glabridin may inhibit formation of foam cells via downregulating the phosphorylation of p38, ERK and JNK. This indicated that protein kinase inhibitors could be used as potential therapeutic agents for the prevention and treatment of vascular barrier dysfunction and endothelial permeability.

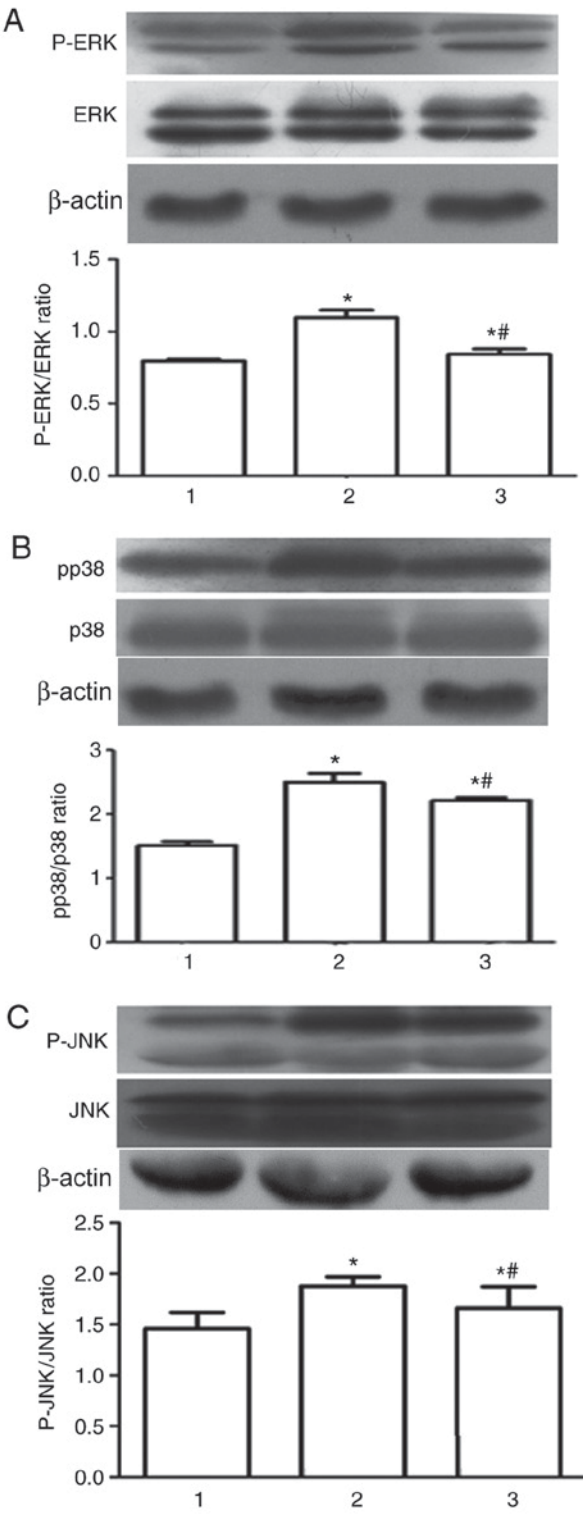

Figure 5. The effects of Glabridin on the activation of MAPK Signaling pathway. Phosphorylation of (A) ERK, (B) p38 and (C) JNK indicated by western blot images and bar graphs of protein quantification. *P<0.05 vs. 1; #P<0.05 vs. 2. 1, normal group; 2, model group; 3, Glabridin group; MLCK, myosin light chain kinase; MAPK, mitogen-activated protein kinase; MLC, myosin light chain; ERK, extracellular signal-regulated kinase; JNK, c-Jun N-terminal kinase; p, phosphorylated.

MAP kinase (ERK1 and ERK2) affects movement mechanism of cells through phosphorylation, and enhances MLCK activity, leading to MLC phosphorylation, cell junction disruption and cell gap formation (34). Inhibition of MAPK activity results in decreased MLCK function, decreased MLC phosphorylation and decreased cell migration in the extracellular matrix. However, increased activity of MAPK kinase leads to activation of MAPK, resulting in phosphorylation of MLCK and MLC, and enhanced cell migration (35). MAPK is able to phosphorylate MLCK directly, increasing its ability to phosphorylate MLC, which promotes cytoskeleton contraction necessary for cell movement (35,36). MLCK, encoded by the MLCK 1-3 gene located on the human chromosome 3,20,16 (12), contains multiple phosphorylation sites of MAP kinase. Previous studies have demonstrated that MLCK, a key regulator of cell movement and contraction, is a MAPK substrate (34,37). Notably, ERK1 and ERK2 can directly phosphorylate MLCK *in vitro*, leading to enhanced phosphorylation of MLC (34). This phosphorylation was associated with increased sensitivity to Ca^{2+}/CaM. In addition to the MAPK signaling pathway, MLC serves an important role in myosin function through Ca^{2+}/phospholipid dependent protein kinase II, protein kinase C and cAMP dependent protein kinase (38,39).

In conclusion, the present study demonstrated that Glabridin has effects on the regulation of lipid metabolism disorder, endothelial dysfunction and increased permeability. By downregulating the phosphorylation levels of p38, ERK and JNK, Glabridin inhibits the expression of MLCK and the activity of MLC, MLCK and the formation of foam cells. Therefore, Glabridin may be a potential treatment for atherosclerosis and serve a specific role in the prevention and treatment of increased vascular permeability.

Acknowledgements

Not applicable.

Funding

The present study was supported by National Natural Science Foundation of China (grant nos. 81570419 and 81270372).

Availability of data and materials

The datasets used and/or analyzed during the present study may be obtained at the reasonable request of the respective authors without prejudice to the confidentiality of the participants.

Authors' contributions

HZ designed and organized the study. GW and GS performed the permeability assay, histological examination, immunohistochemistry analysis, reverse transcription-quantitative polymerase chain reaction and Western blotting. YW and PY detected serum lipids. XW assayed endothelial function. BZ analyzed the data and wrote the manuscript.

Ethics approval and consent to participate

The present protocols were approved by the Ethics Committee of Anhui Medical University (Hefei, China).

Patient consent for publication

Not applicable.

Competing interests

The authors declare that they have no competing interests.

References

1. Hansson GK: Inflammation, atherosclerosis, and coronary artery disease. N Engl J Med 352: 1685-1695, 2005.
2. Lusis AJ: Atherosclerosis. Nature 407: 233-241, 2000.
3. Kronenberg F, Kronenberg MF, Kiechl S, Trenkwalder E, Santer P, Oberhollenzer F, Egger G, Utermann G and Willeit J: Role of lipoprotein(a) and apolipoprotein(a) phenotype in atherogenesis. Circulation 100: 1154-1160, 1999.
4. Assmann G, Cullen P, Jossa F, Lewis B and Mancini M: Coronary heart disease: Reducing the risk: The scientific background to primary and secondary prevention of coronary heart disease. A worldwide view. International Task force for the Prevention of Coronary Heart disease. Arterioscl Thromb Vasc Biol 19: 1819-1824, 1999.
5. Lusis AJ, Mar R and Pajukanta P: Genetics of atherosclerosis. Annu Rev Genomics Hum Genet 5: 189-218, 2004.
6. Williams IL, Wheatcroft SB, Shah AM and Kearney MT: Obesity, atherosclerosis and the vascular endothelium: Mechanisms of reduced nitric oxide bioavailability in obese humans. Int J Obes Relat Metab Disord 26: 754-764, 2002.
7. Daiber A, Steven S, Weber A, Shuvaev VV, Muzykantov VR, Laher I, Li H, Lamas S and Münzel T: Targeting vascular (endothelial) dysfunction. Br J Pharmacol 174: 1591-1619, 2017.
8. Hamlat-Khennaf N, Neggazi S, Ayari H, Feugier P, Bricca G, Aouichat-Bouguerra S and Beylot M: Inflammation in the perivascular adipose tissue and atherosclerosis. C R Biol 340: 156-163, 2017 (In French).
9. Quiros M and Nusrat A: RhoGTPases, actomyosin signaling and regulation of the epithelial apical junctional complex. Semin Cell Dev Biol 36: 194-203, 2014.
10. Petrache I, Birukov K, Zaiman AL, Crow MT, Deng H, Wadgaonkar R, Romer LH and Garcia JG: Caspase-dependent cleavage of myosin light chain kinase (MLCK) is involved in TNF-alpha-mediated bovine pulmonary endothelial cell apoptosis. FASEB J 17: 407-416, 2003.
11. Miao W, Wu X, Wang K, Wang W, Wang Y , Li Z, Liu J, Li L and Peng L: Sodium butyrate promotes reassembly of tight junctions in caco-2 monolayers involving inhibition of MLCK/MLC2 pathway and phosphorylation of PKCβ2. Int J Mol Sci 17: 1696-1708, 2016.
12. Stull JT, Kamm KE and Vandenboom R: Myosin light chain kinase and the role of myosin light chain phosphorylation in skeletal muscle. Arch Biochem Biophys 510: 120-128, 2011.
13. Brasier AR: The nuclear factor-kappaB-interleukin-6 signalling pathway mediating vascular inflammation. Cardiovasc Res 86: 211-218, 2010.
14. Yokota T, Nishio H, Kubota Y and Mizoguchi M: The inhibitory effect of glabridin from licorice extracts on melanogenesis and inflammation. Pigment Cell Res 11: 355-361, 1998.
15. Simmler C, Pauli GF and Chen SN: Phytochemistry and biological properties of glabridin. Fitoterapia 90: 160-184, 2013.
16. Cui YM, Ao MZ, Li W and Yu LJ: Effect of Glabridin from Glycyrrhiza glabra on Learning and Memory in Mice. Planta Med 74: 377-380, 2008.
17. Hu ZP, Fang XL, Fang N, Wang XB, Qian HY, Cao Z, Cheng Y, Wang BN and Wang Y: Melatonin ameliorates vascular endothelial dysfunction, inflammation, and atherosclerosis by suppressing the TLR4/NF-κB system in high-fat-fed rabbits. J Pineal Res 55: 388-398, 2013.
18. Zhang C, Zheng H, Yu Q, Yang P, Li Y, Cheng F, Fan J and Liu E: A practical method for quantifying atherosclerotic lesions in rabbits. J Comp Pathol 142: 122-128, 2010.
19. Wang H, Zhu HQ, Feng W, Zhou Q, Gui SY and Yuan W: MicroRNA-1 prevents high-fat diet-induced endothelial permeability in apoE knock-out mice. Mol Cell Biochem 378: 153-159, 2013.
20. Zhou B, Pan Y, Hu Z, Wang X, Han J, Zhou Q, Zhai Z and Wang Y: All-trans-retinoic acid ameliorated high fat diet-induced atherosclerosis in rabbits by inhibiting platelet activation and inflammation. J Biomed Biotechnol 2012: 259693, 2012.
21. Livak KJ and Schmittgen TD: Analysis of relative gene expression data using real-time quantitative PCR and the 2 (-Delta Delta C(T)) method. Methods 25: 402-408, 2001.
22. Agil A, Navarro-Alarcón M, Ruiz R, Abuhamadah S, El-Mir MY and Vázquez GF: Beneficial effects of melatonin on obesity and lipid profile in young Zucker diabetic fatty rats. J Pineal Res 50: 207-212, 2011.
23. Liuzzo G: Atherosclerosis: An inflammatory disease. Rays 26: 221-230, 2001.
24. Fatkhullina AR, Peshkova IO and Koltsova EK: The role of cytokines in the development of atherosclerosis. Biochemistry (Mosc) 81: 1358-1370, 2016.
25. Libby P: Inflammation in atherosclerosis. Arterioscler Thromb Vasc Biol 32: 2045-2051, 2012.
26. Corre I, Paris F and Huot J: The p38 pathway, a major pleiotropic cascade that transduces stress and metastatic signals in endothelial cells. Oncotarget 8: 55684-55714, 2017.
27. Yanni AE: The laboratory rabbit: An animal model of atherosclerosis research. Lab Anim 38: 246-256, 2004.
28. Bocan TM, Mueller SB, Mazur MJ, Uhlendorf PD, Brown EQ and Kieft KA: The relationship between the degree of dietary-induced hypercholesterolemia in the rabbit and atherosclerotic lesion formation. Atherosclerosis 102: 9-22, 1993.
29. Urbano RL, Furia C, Basehore S and Clyne AM: Stiff substrates increase inflammation-induced endothelial monolayer tension and permeability. Biophys J 113: 645-655, 2017.
30. Bryk D, Olejarz W and Zapolska-Downar D: Mitogen-activated protein kinases in atherosclerosis. Postepy Hig Med Dosw (Online) 68: 10-22, 2014 (In Polish).
31. Hao XZ and Fan HM: Identification of miRNAs as atherosclerosis biomarkers and functional role of miR-126 in atherosclerosis progression through MAPK signalling pathway. Eur Rev Med Pharmacol Sci 21: 2725-2733, 2017.
32. Wagner EF and Nebreda AR: Signal integration by JNK and p38 MAPK pathways in cancer development. Nat Rev Cancer 9: 537-549, 2009.
33. Harding A, Cortez-Toledo E, Magner NL, Beegle JR, Coleal-Bergum DP, Hao D, Wang A, Nolta JA and Zhou P: Highly efficient differentiation of endothelial cells from pluripotent stem cells requires the MAPK and the PI3K pathways. Stem Cells 35: 909-919, 2017.
34. Zuo L, Yang X, Lu M, Hu R, Zhu H, Zhang S, Zhou Q, Chen F, Gui S and Wang Y: All-trans retinoic acid inhibits human colorectal cancer cells RKO migration via downregulating myosin light chain kinase expression through MAPK signaling pathway. Nutr Cancer 68: 1225-1233, 2016.
35. Sellers JR and Adelstein RS: Regulation of contractile activity. In: Enzymes. Tamanoi F (ed). Vol 18. 3rd edition. Academic press, New York, NY, pp381-418, 1987.
36. Tan JL, Ravid S and Spudich JA: Control of nonmuscle myosins by phosphorylation. Annu Rev Biochem 61: 721-759, 1992.
37. Wang B, Yan Y, Zhou J, Zhou Q, Gui S and Wang Y: A novel all-trans retinoid acid derivatives inhibits the migration of breast cancer cell lines MDA-MB-231 via myosin light chain kinase involving p38-MAPK pathway. Biomed Pharmacother 67: 357-362, 2013.
38. Ringvold HC and Khalil RA: Protein kinase C as regulator of vascular smooth muscle function and potential target in vascular disorders. Adv Pharmacol 78: 203-301, 2017.
39. Yu T, Wang Y, Qian D, Sun X, Tang Y, Shen X and Lin L: Advanced glycation end products impair Ca2+ mobilization and sensitization in colonic smooth muscle cells via the CAMP/PKA pathway. Cell Physiol Biochem 43: 1571-1587, 2017.